Computing 56, 237–258 (1996)

Computing

Parallel Solvers for Linear and Nonlinear Exterior Magnetic Field Problems Based upon Coupled FE/BE Formulations*

B. Heise and **M. Kuhn**, Linz

Received January 25, 1995; revised June 2, 1995

Abstract — Zusammenfassung

Parallel Solvers for Linear and Nonlinear Exterior Magnetic Field Problems Based upon Coupled FE/BE Formulations. An efficient parallel algorithm for solving linear and nonlinear exterior boundary value problems arising, e.g., in magnetostatics is presented. It is based upon the domain-decomposition-(DD)-coupling of Finite Element and Galerkin Boundary Element Methods which results in a unified variational formulation. In this way, e.g., magnetic field problems in an unbounded domain with Sommerfeld's radiation condition can be modelled correctly. The problem of a nonsymmetric system matrix due to Galerkin-BEM is overcome by transforming it into a symmetric but indefinite matrix and applying Bramble/Pasciak's CG for indefinite systems. For preconditioning, the main ideas of recent DD research are being applied. Test computations on a multiprocessor system were performed for two problems of practical interest including a nonlinear example.

AMS Subject Classification: 65N55, 65N30, 65N22, 65N38, 78A30

Key words: Nonlinear partial differential equations, domain decomposition, boundary element methods, finite element methods, coupling, magnetic field calculations.

Parallele Lösungsstrategien für lineare und nichtlineare Außenraum-Magnetfeldprobleme auf der Grundlage gekoppelter Finite Elemente/Randelemente-Formulierungen. In der vorliegenden Arbeit wird ein effizienter paralleler Algorithmus zur Lösung linearer und nichtlinearer Außenraumprobleme, wie sie z.B. in der Magnetostatik auftreten, beschrieben. Er basiert auf der Kopplung der Finite Elemente Methode mit der Galerkin-Randelementmethode mit Hilfe von Gebietszerlegungstechniken über eine einheitliche Variationsformulierung. Auf diese Weise können z.B. Magnetfeldprobleme mit der Sommerfeldschen Abstrahlbedingung vollständig modelliert werden. Die durch die Galerkin-Randelementmethode entstehende nichtsymmetrische Matrix wird in eine symmetrische indefinite Matrix transformiert, um Bramble/Pasciak's CG-Verfahren für indefinite Systeme anzuwenden. Zur Vorkonditionierung werden die neuesten Resultate auf dem Gebiet der Gebietszerlegungsmethoden genutzt. Numerische Resultate, die für zwei praktisch interessante Probleme, darunter ein nichtlineares, auf einem Mehrprozessorsystem erhalten wurden, werden diskutiert.

1. Introduction

Recently, domain decomposition (DD) methods have found growing interest. One main reason is the rising application of Multiple Instruction Multiple Data

* This research has been supported by the German Research Foundation DFG within the Priority Research Programme "Boundary Element Methods" under Grant La 767/1-3.

(MIMD) parallel computers [2, 4, 5, 9, 18]. The DD methods with their inherent parallel data distribution allow parallel computations with low communication effort. Thus, computing on hundreds of processors can be performed with high efficiency [25, 27].

One motivation for developing fast and parallel field simulation methods is the use in parallel optimization programs for solving optimal design problems, e.g., for electric machines [19]. In general, iterative algorithms which are based on solving linear systems in each iteration step benefit extraordinary from fast parallel linear solvers and minor improvements of the latter can lead to a remarkable decrease of computation time required for solving the original problem.

Another important aspect is that DD methods allow us to "marry" the advantages of the Finite Element Method (FEM) to those of the Boundary Element Method (BEM) via a unified variational formulation [6, 29–31, 35].

Indeed, certain phenomena, e.g., problems arising in solid mechanics, electric and magnetic fields can be described by partial differential equations which are given over unbounded domains. Due to a rather complicated structure in some bounded subdomain they can be modelled correctly neither by a pure FEM, nor by a pure BEM approach. Therefore there is a need for coupling both methods. As an example, in the magnetic field computations for electric machines, we can use BEM for the infinite exterior subdomain of the machine more successfully than the FEM, which is preferred for the subdomains in the interior of the machine due to complicated structure, currents, and nonlinearities occurring there [25, 27, 29–31]. In this paper, we extend the DD coupling approach given in [30, 31] to the coupling of finite element (f.e.), interior boundary element (b.e.) and exterior b.e. subdomains. We present the unified variational formulation for linear problems and propose a discretization method.

The resulting system of equations is solved by a parallel preconditioned CG (PCG) method [10, 13] which is intended for running on a parallel computer with message-passing principle using a distributed data structure. We apply Bramble/Pasciak's CG for indefinite systems [1] as well as the essential ideas of recent DD research [3, 13, 15, 32–34]. Efficiency and scale-up results for the parallel algorithm can be found in [25, 27]. For the preconditioning of problems in unbounded domains new ideas are necessary.

The remainder of the paper is organized as follows. In Section 2 we describe the problem class considered and introduce a coupled f.e./b.e. domain decomposition of an infinite domain. In Section 3 we present the basic integral equations for both exterior and interior subdomains. In Section 4 the unifying f.e./b.e. weak formulation is established. In Section 5 we present the system of equations resulting from the discretization. In the case of circular coupling boundaries of b.e. subdomains we may obtain circulant local matrices which can be handled

with FFT. Section 6 is devoted to the parallel solver. We perform the transformation into a self-adjoint discrete operator and give relevant spectral equivalence results. We present an improved parallel CG algorithm which allows a better synchronization between FEM and BEM processors than the straightforward implementation of the BEM part based on [13]. As an application, we describe the handling of nonlinear problems by Newton's method in Section 7. Finally, in Section 8 we present field calculations for linear and nonlinear problems, including the computation of magnetic inductions at arbitrary points of the exterior subdomain, which is a problem of practical importance, and add some concluding remarks.

2. Exterior Boundary Value Problems

Several classes of practical problems are characterized by the fact that the differential equation arising as a result of modelling the problem has to be satisfied over an unbounded domain. On the other hand one can usually observe that phenomena as nonlinearities, sources and sinks are restricted to a bounded region whereas the equation becomes linear and homogeneous in the unbounded exterior domain. We are going to investigate the latter class of problems as they arise, for example, in magnetostatics and restrict ourselves to 2d-problems by considering a characteristical cross-section, which lies in the (x, y)-plane of the $\mathbf{R}^3$, of the original electromagnetic device which is to be modelled.

Let us assume that Ω_0 is a bounded simply connected domain and that we are given homogeneous Dirichlet boundary conditions on $\Gamma_D = \partial\Omega_0$. Formally the linear magnetic field problem can be written as follows [24]

$$-\operatorname{div}\left(\nu(x)\,\nabla u(x)\right) = S(x) + \frac{\partial H_{0y}(x)}{\partial x} - \frac{\partial H_{0x}(x)}{\partial y}, \quad x \in \Omega := R^2 \setminus \overline{\Omega}_0 \tag{1}$$

$$u(x) = 0, \quad x \in \Gamma_D \tag{2}$$

$$|u(x)| \to 0 \quad \text{for } |x| \to \infty. \tag{3}$$

Then the solution u is the z-component of some vector potential. The component of the current density, which acts orthogonal to the cross-section being considered, is represented by $S(x)$, H_{0x} and H_{0y} stand for sources associated with permanent magnets that may occur and $\nu(.)$ denotes a material-dependent coefficient. For more details of the physical model developed from Maxwell's equations we refer to [22, 24].

Now we introduce the exterior domain Ω_+ by defining a, so called, coupling boundary $\Gamma_+ =: \partial\Omega_+$. The definition of Γ_+ is being restricted by the conditions

$$\nu(x) = \nu_p \;\; \forall x \in \Omega_+, \left(\operatorname{supp} S(x) \cup \operatorname{supp} H_0(x)\right) \subset \overline{\Omega}_-, \quad \operatorname{diam}\left(\overline{\Omega}_0 \cup \overline{\Omega}_-\right) < 1, \tag{4}$$

where $\Omega_- := R^2 \setminus (\overline{\Omega}_+ \cup \overline{\Omega}_0)$. Note that the condition $\operatorname{diam}(\overline{\Omega}_0 \cup \overline{\Omega}_-) < 1$ is only technical and can be fulfilled by scaling the problem appropriately.

Besides the decomposition $\overline{\Omega} = \overline{\Omega}_- \cup \overline{\Omega}_+$ performed above we allow the inner domain Ω_- to be decomposed further following the natural given decomposition of Ω_- according to the change of the coefficients $\nu(x)$

$$\overline{\Omega}_- = \bigcup_{j=1}^{N_M} \overline{\hat{\Omega}}_j, \quad \text{with} \quad \hat{\Omega}_i \cap \hat{\Omega}_j = \emptyset \; \forall i \neq j. \tag{5}$$

The final substructuring into non-overlapping subdomains Ω_i, $i \in \mathcal{I} := \{1, \ldots, p\}$ can now be defined as follows

$$\overline{\Omega} = \bigcup_{i \in \mathcal{I}} \overline{\Omega}_i, \text{ where } \Omega_p := \Omega_+ \quad \text{and} \quad \overline{\hat{\Omega}}_j = \bigcup_{i \in \mathcal{I}_j} \overline{\Omega}_i \; \forall j = 1, \ldots, N_M \tag{6}$$

with index sets fulfilling

$$\mathcal{I}_j \subset \mathcal{I}^\star := \{1, \ldots, p-1\}, \; \bigcup_{j=1}^{N_M} \mathcal{I}_j = \mathcal{I}^\star, \quad \mathcal{I}_j \cap \mathcal{I}_k = \emptyset \; \forall j \neq k,$$

that is the subdomains $\hat{\Omega}_j$ determined by the materials may be decomposed further (cf. [11, 13, 14]). Looking at the example presented in Section 8.4 (electromagnet, Fig. 3) we may introduce a circle as coupling boundary Γ_+ to obtain Ω_+ (domain VIII) and Ω_- (union of the domains I–VII). Naturally we are given a decomposition of Ω_- into four subdomains (I, II, III, IV–VII). In our computations we use a decomposition of Ω_- into 7 subdomains, that is $\mathcal{I}^\star = \{1, \ldots, 7\}$, as it is shown in Fig. 3.

We assume that there exist open balls $B_{\underline{r}_i}$ and $B_{\bar{r}_i}$ ($i \in \mathcal{I}^\star$) with positive radii $\underline{r}_i$ and $\bar{r}_i$, such that

$$B_{\underline{r}_i} \subset \Omega_i \subset B_{\bar{r}_i} \quad \text{and} \quad 0 < \underline{c} \leq \frac{\bar{r}_i}{\underline{r}_i} \leq \bar{c} \; \forall i \in \mathcal{I}^\star \tag{7}$$

with fixed (i-independent) constants $\underline{c}$ and $\bar{c}$. Note that in the following we omit the x-dependence of the material function $\nu(x)$ and assume that it is constant over the subdomains, i.e.

$$\nu(x) =: \nu_i \; \forall x \in \Omega_i \; (i \in \mathcal{I}).$$

The decomposition of Ω implies coupling conditions which have to be satisfied. Formally we have

$$u_i(x) = u_j(x) \quad \text{and} \quad \nu_i \frac{\partial u_i(x)}{\partial n} = -\nu_j \frac{\partial u_j(x)}{\partial n}; \; x \in \Gamma_{ij} := \overline{\Omega}_i \cap \overline{\Omega}_j \; (i, j \in \mathcal{I}^\star) \tag{8}$$

where the indices i, j stand for the trace-operator associated with the subdomains Ω_i and Ω_j, respectively, applied to the according function and n is the normal outward direction with respect to the subdomains. Since we define the normal direction associated with Ω_+ still as outward direction with respect to Ω_- we have a change of signs if $\Omega_+ = \Omega_p$ is involved

$$u_i(x) = u_p(x) \text{ and } \nu_i \frac{\partial u_i(x)}{\partial n} = \nu_p \frac{\partial u_p(x)}{\partial n};\ x \in \Gamma_{ip} := \overline{\Omega}_i \cap \overline{\Omega}_p \ (\forall i: \Gamma_i \cap \Gamma_p \neq \emptyset) \tag{9}$$

Finally, we define two disjoint sets of indices $\mathcal{I}_F$ and $\mathcal{I}_B$, such that $\mathcal{I}_F \cup \mathcal{I}_B = \mathcal{I}$, $p \in \mathcal{I}_B$ and

$$(\operatorname{supp} S(x) \cup \operatorname{supp} H_0(x)) \cap \Omega_i = \emptyset \quad \forall i \in \mathcal{I}_B.$$

For each Ω_i $(i \in \mathcal{I})$ the index i belongs to one of the two index sets $\mathcal{I}_B$ and $\mathcal{I}_F$ according to the discretization method applied to Ω_i, where $\mathcal{I}_B$ and $\mathcal{I}_F$ stand for BEM and FEM, respectively.

3. Integral Operators

The decomposition of the original domain Ω into subdomains (6) leads to subproblems defined over Ω_i $(i \in \mathcal{I})$ which are connected by the coupling conditions (8), (9). We want to focus our interest on the unbounded domain $\Omega_+ = \Omega_p$. It is well known that, using integral equations, one can restrict the problem to data on the boundary $\partial\Omega_+ = \Gamma_+$. In order to apply the method of integral equations one has to know the fundamental solution of the according differential operator L. This function is well known for $L = -\Delta = -\operatorname{div}\operatorname{grad}$, in particular we have in the 2d-case $E(x, y) = -\ln|x-y|/2\pi$. A first important equation is the representation formula for $x \in \Omega_+$

$$u(x) = \int_{\Gamma_+} \left[\frac{\partial}{\partial n_y} E(x, y) u(y) - E(x, y) \frac{\partial}{\partial n_y} u(y) \right] ds_y \quad x \in \Omega_+. \tag{10}$$

Interpreting the right hand side in (10) as a combination of a single and double layer potential, and using well known properties [17] one can derive the Calderon equation

$$\begin{pmatrix} u \\ \lambda \end{pmatrix} = \mathbf{C}_+ \begin{pmatrix} u \\ \lambda \end{pmatrix} := \begin{pmatrix} \frac{1}{2} I_p + K_p & -V_p \\ -D_p & \frac{1}{2} I_p - K_p' \end{pmatrix} \begin{pmatrix} u \\ \lambda \end{pmatrix}, \tag{11}$$

with $\lambda = \partial u / \partial n$ being the normal derivative of u, I the identity operator and $\mathbf{C}_+$ being the Calderon-projector. Note that n_x, n_y denote the outward normal direction with respect to Ω_-. The operators K, V, D are defined for Lipschitz

domains Ω_i $(i \in \mathcal{I}_B)$ with the boundary $\partial\Omega_i$ as follows

$$(V_i\lambda)(x) = \int_{\partial\Omega_i} E(x, y)\lambda(y)\, ds_y$$

$$(K_i u)(x) = \int_{\partial\Omega_i} \frac{\partial}{\partial n_y} E(x, y)u(y)\, ds_y$$

$$(K_i'\lambda)(x) = \int_{\partial\Omega_i} \frac{\partial}{\partial n_x} E(x, y)\lambda(y)\, ds_y$$

$$(D_i u)(x) = -\frac{\partial}{\partial n_x} \int_{\partial\Omega_i} \frac{\partial}{\partial n_y} E(x, y)u(y)\, ds_y. \tag{12}$$

Thus, we have established equations describing the boundary data u and λ. Interior problems can be handled in an analogous way to exterior problems. The Calderon equation reads for inner domains $(i \in \mathcal{I}_B \setminus \{p\})$

$$\begin{pmatrix} u \\ \lambda \end{pmatrix} = \mathbf{C}_i \begin{pmatrix} u \\ \lambda \end{pmatrix} := \begin{pmatrix} \frac{1}{2}I_i - K_i & V_i \\ D_i & \frac{1}{2}I_i + K_i' \end{pmatrix} \begin{pmatrix} u \\ \lambda \end{pmatrix}. \tag{13}$$

The change of signs arises from the definition of the normal direction. The mapping properties of the operators V_i, D_i, K_i, K_i' are well known [7], [8].

4. The Weak Formulation

Because of the conditions we have forced on Ω_i for $i \in \mathcal{I}_B$ we can apply the boundary element method to these domains whereas the remaining subdomains Ω_i $(i \in \mathcal{I}_F)$ are being handled as FEM domains so that currents, permanent magnetizations or nonlinearities (cf. Section 7) can be covered easily.

In order to obtain a bilinear form and finally our weak formulation we follow the usual Galerkin-procedure and multiply the differential equation (1) by a test function $v(.)$ and integrate by parts

$$\sum_{i \in \mathcal{I}} \left[\int_{\Omega_i} \nu_i \nabla^T u(x)\, \nabla v(x)\, dx - \int_{\Gamma_i} \nu_i \frac{\partial u(x)}{\partial n} v(x)\, ds \right]$$

$$= \sum_{i \in \mathcal{I}_F} \int_{\Omega_i} \left[\mathrm{S}(x) + \frac{\partial \mathrm{H}_{0\mathrm{y}}(x)}{\partial \mathrm{x}} - \frac{\partial \mathrm{H}_{0\mathrm{x}}(x)}{\partial \mathrm{y}} \right] v(x)\, dx. \tag{14}$$

We note that the right hand side vanishes in Ω_i for $i \in \mathcal{I}_B$. Because the coupling conditions (8), (9) have to be satisfied the integrals over Γ_{ij} cancel out for $i, j \in \mathcal{I}_F$ and new integrals over Γ_{ij} for $i, j \in \mathcal{I}_B$ can be inserted to give the

following equation

$$\sum_{i\in\mathcal{I}_F}\int_{\Omega_i}\nu_i\nabla^T u(x)\nabla v(x)\,dx+\sum_{i\in\mathcal{I}_B\setminus\{p\}}\int_{\Gamma_i}\nu_i\frac{\partial}{\partial n}u(x)v(x)\,ds$$

$$-\int_{\Gamma_+}\nu_p\frac{\partial}{\partial n}u(x)v(x)\,ds$$

$$=\sum_{i\in\mathcal{I}_F}\int_{\Omega_i}\left[S(x)v(x)-H_{0y}(x)\frac{\partial v(x)}{\partial x}+H_{0x}(x)\frac{\partial v(x)}{\partial y}\right]dx. \quad (15)$$

Now, using (11) and (13), the normal derivative of u can be replaced. In order to obtain a symmetric form we also use the second identity from the Calderon equation and insert additional terms which add up to zero. Thus, we have to solve the following weak formulation.

Find $(\lambda, u)\in\mathbf{V}:=\Lambda\times\mathbf{U}_0$:

$$a(\lambda,u;\eta,v)=\langle F,v\rangle\quad\forall(\eta,v)\in\mathbf{V}, \quad (16)$$

where

$$a(\lambda,u;\eta,v):=a_B(\lambda,u;\eta,v)+a_F(u,v)$$

$$a_B(\lambda,u;\eta,v):=\sum_{i\in\mathcal{I}_B\setminus\{p\}}\nu_i\{\langle D_iu_i,v_i\rangle_{\Gamma_i}+\tfrac{1}{2}\langle\lambda_i,v_i\rangle_{\Gamma_i}+\langle\lambda_i,K_iv_i\rangle_{\Gamma_i}$$
$$+\langle\eta_i,V_i\lambda_i\rangle_{\Gamma_i}-\langle\eta_i,K_iu_i\rangle_{\Gamma_i}-\tfrac{1}{2}\langle\eta_i,u_i\rangle_{\Gamma_i}\}$$
$$+\nu_p\{\langle D_pu_p,v_p\rangle_{\Gamma_+}-\tfrac{1}{2}\langle\lambda_p,v_p\rangle_{\Gamma_+}+\langle\lambda_p,K_pv_p\rangle_{\Gamma_+}$$
$$+\langle\eta_p,V_p\lambda_p\rangle_{\Gamma_+}-\langle\eta_p,K_pu_p\rangle_{\Gamma_+}+\tfrac{1}{2}\langle\eta_p,u_p\rangle_{\Gamma_+}\}$$

$$a_F(u,v):=\sum_{i\in\mathcal{I}_F}\nu_i\int_{\Omega_i}\nabla^T u(x)\nabla v(x)\,dx$$

$$\langle F,v\rangle:=\sum_{i\in\mathcal{I}_F}\int_{\Omega_i}\left[S(x)v(x)-H_{0y}(x)\frac{\partial v(x)}{\partial x}+H_{0x}(x)\frac{\partial v(x)}{\partial y}\right]dx$$

$$\langle\lambda_i,v_i\rangle_{\Gamma_i}:=\int_{\Gamma_i}\lambda_iv_i\,ds\ \text{and}\ v_i=v|_{\partial\Omega_i},\ u_i=u|_{\partial\Omega_i}.$$

Let the spaces $\mathbf{U}_0$ and Λ be defined as follows:

$$\mathbf{U}_0:=\{u\in H^1(\Omega_-):u|_{\Gamma_{BE}}\in H^{1/2}(\Gamma_{BE}),\ u|_{\partial\Omega_0}=0\}$$
$$\Lambda:=\prod_{i\in\mathcal{I}_B}H^{-1/2}(\Gamma_i),$$

where $\Gamma_{BE}:=\bigcup_{i\in\mathcal{I}_B}\partial\Omega_i\setminus\Gamma_D$, $\Gamma_{FE}:=\bigcup_{i\in\mathcal{I}_F}\partial\Omega_i\setminus\Gamma_D$, $\Gamma_C:=\Gamma_{BE}\cup\Gamma_{FE}$. In $\mathbf{V}$, we consider the norm with $\Omega_F:=\bigcup_{i\in\mathcal{I}_F}\Omega_i$:

$$\|(\lambda,u)\|_{\mathbf{V}}:=\left(\|\lambda\|_{\Lambda}^2+\|u\|_{H^{1/2}(\Gamma_{BE})}^2+\|u\|_{H^1(\Omega_F)}^2\right)^{1/2}.$$

Note, for $\mathcal{I}_F = \emptyset$ we obtain a pure BEM model. The number p stands for both, the number of subdomains and the number of processors being used, where the subdomains are mapped onto the p processors of the MIMD computer in a one-to-one relation.

The bilinear form $a(.;.)$ is **V**-elliptic and **V**-bounded (cf. [28] for BEM domain decomposition) under the conditions (2), (4), (7) imposed on the domain decomposition, and existence and uniqueness of the solution of (16) are a direct consequence of the Lax-Milgram lemma.

5. The Discrete Problem

Now, we can define the nodal FE/BE-basis of piecewise linear trial functions based upon a regular triangulation of the subdomains Ω_i, $i \in \mathcal{I}_F$ and the according discretization of the boundary pieces $\Gamma_{ij} = \overline{\Omega}_i \cap \overline{\Omega}_j$, $i, j \in \mathcal{I}$:

$$\Phi = \left[\phi_1, \ldots, \phi_{N_\Lambda}, \phi_{N_\Lambda+1}, \ldots, \phi_{N_\Lambda+N_C}, \phi_{N_\Lambda+N_C+1}, \ldots, \phi_N\right],$$

where $N = N_\Lambda + N_C + N_I$ and $N_I = \sum_{i \in \mathcal{I}_F} N_{I,i}$, $N_\Lambda = \sum_{i \in \mathcal{I}_B} N_{\Lambda,i}$. Here, $\phi_1, \ldots, \phi_{N_\Lambda}$ are the basis functions for approximating λ on Γ_{BE}, $\phi_{N_\Lambda+1}, \ldots, \phi_{N_\Lambda+N_C}$ represent u on $\partial\Omega_i$, $i \in \mathcal{I}$, and $\phi_{N_\Lambda+N_C+1}, \ldots, \phi_{N_\Lambda+N_C+N_I}$ approximate u in Ω_i, $i \in \mathcal{I}_F$. The definition of the finite dimensional subspaces of Λ, $\mathbf{U}_0$ and $\mathbf{V}$

$$\begin{aligned}
\Lambda_h &:= \operatorname{span}\left[\phi_1, \phi_2, \ldots, \phi_{N_\Lambda}\right],\\
\mathbf{U}_h &:= \operatorname{span}\left[\phi_{N_\Lambda+1}, \ldots, \phi_{N_\Lambda+N_C}, \phi_{N_\Lambda+N_C+1}, \ldots, \phi_N\right],\\
\mathbf{V}_h &:= \Lambda_h \times \mathbf{U}_h
\end{aligned}$$

allows us to formulate the discrete problem as follows:
Find $u_h \in \mathbf{V}_h$ such that

$$a(u_h, v_h) = \langle F, v_h \rangle \quad \forall v_h \in \mathbf{V}_h. \tag{17}$$

The isomorphism Φ: $\mathbf{R}^N \to \mathbf{V}_h$ leads to the linear system:

$$\begin{pmatrix} K_\Lambda & -K_{\Lambda C} & 0 \\ K_{C\Lambda} & K_C & K_{CI} \\ 0 & K_{IC} & K_I \end{pmatrix} \begin{pmatrix} \mathbf{u}_\Lambda \\ \mathbf{u}_C \\ \mathbf{u}_I \end{pmatrix} = \begin{pmatrix} \mathbf{f}_\Lambda \\ \mathbf{f}_C \\ \mathbf{f}_I \end{pmatrix}, \tag{18}$$

where the block entries are defined by

$$(K_\Lambda \mathbf{u}_\Lambda, \mathbf{v}_\Lambda) = \sum_{i \in \mathcal{I}_B} \nu_i \langle \eta_i, V_i \lambda_i \rangle_{\Gamma_i},$$

where $\lambda_i = \Phi_{\Lambda_i} \mathbf{u}_{\Lambda_i}$, $\eta_i = \Phi_{\Lambda_i} \mathbf{v}_{\Lambda_i}$,

$$\begin{aligned}
(K_{C\Lambda} \mathbf{u}_\Lambda, \mathbf{v}_C) = &\sum_{i \in \mathcal{I}_B \setminus \{p\}} \nu_i \left\{ \langle \lambda_i, K_i v_i \rangle_{\Gamma_i} + \tfrac{1}{2} \langle \lambda_i, v_i \rangle_{\Gamma_i} \right\} \\
&+ \nu_p \left\{ \langle \lambda_p, K_p v_p \rangle_{\Gamma_p} - \tfrac{1}{2} \langle \lambda_p, v_p \rangle_{\Gamma_p} \right\},
\end{aligned}$$

where $\lambda_i = \Phi_{\Lambda_i}\mathbf{u}_{\Lambda_i}$, $v_i = \Phi_{C_i}\mathbf{v}_{C_i}$,

$$K_{\Lambda C} = K_{C\Lambda}^T$$

$$K_C = K_{CB} + K_{CF}, \text{ where}$$

$$(K_{CB}\mathbf{u}_C, \mathbf{v}_C) = \sum_{i \in \mathcal{I}_B} \nu_i \langle D_i u_i, v_i \rangle_{\Gamma_i},$$

$$u_i = \Phi_{C_i}\mathbf{u}_{C_i},\ v_i = \Phi_{C_i}\mathbf{v}_{C_i},$$

$$\left(\begin{pmatrix} K_{CF} & K_{CI} \\ K_{IC} & K_I \end{pmatrix} \begin{pmatrix} \mathbf{u}_C \\ \mathbf{u}_I \end{pmatrix}, \begin{pmatrix} \mathbf{v}_C \\ \mathbf{v}_I \end{pmatrix} \right) = \sum_{i \in \mathcal{I}_F} \int_{\Omega_i} \nu(x) \nabla^T u \nabla v \, dx,$$

$$\text{where } u|_{\Omega_F} = \Phi_F \mathbf{u}_F,\ v|_{\Omega_F} = \Phi_F \mathbf{v}_F.$$

Here Φ_{Λ_i} $(i \in \mathcal{I}_B)$ and Φ_{C_i} $(i \in \mathcal{I})$ contain the basis functions for approximating λ and u on $\partial\Omega_i$, respectively. The basis functions in Φ_F are used to approximate u in Ω_i $(i \in \mathcal{I}_F)$.

The f.e. entries, especially K_I, are sparse matrices, whereas the b.e. blocks are fully populated in the general case. We can overcome this drawback if a circle is chosen as coupling boundary Γ_+. If this circle is discretized uniformly into N_B elements then the local discrete b.e. operators become circulant matrices. In this case any matrix-times-vector operation, as it occurs in iterative solution algorithms can be performed by FFT-operations since

$$A = N_B^{-1} F \Lambda F^*, \tag{19}$$

where F is the operator of the discrete Fourier transformation and Λ is a diagonal matrix containing the eigenvalues of A, holds for circulant matrices A. In the case of $N_B = 2^m$ the arithmetical effort can be reduced from $\mathcal{O}(N_B^2)$ to $\mathcal{O}(N_B \ln N_B)$.

In particular we have the following eigenvalues for the discrete operators associated with V_p, D_p and $\tilde{K}_p := K_p - \frac{1}{2} I_p$ [32]

$$\lambda_{V_p,j} = \begin{cases} r|\ln r|h & j = 1 \\ \frac{1}{2}h^2 r \left(\dfrac{\sin \pi s}{\pi} \right)^4 \displaystyle\sum_{k=0}^{\infty} \left\{ \frac{1}{(s+k)^5} + \frac{1}{(1-s+k)^5} \right\} & j = 2, \ldots, N_B \end{cases}$$

$$\lambda_{D_p,j} = \begin{cases} 0 & j = 1 \\ \dfrac{1}{2r} \left(\dfrac{\sin \pi s}{\pi} \right)^4 \displaystyle\sum_{k=0}^{\infty} \left\{ \frac{1}{(s+k)^3} + \frac{1}{(1-s+k)^3} \right\} & j = 2, \ldots, N_B \end{cases}$$

$$\lambda_{\tilde{K}_p,j} = \begin{cases} -h & j = 1 \\ -\frac{1}{2}h \left(\dfrac{\sin \pi s}{\pi} \right)^4 \displaystyle\sum_{k=0}^{\infty} \left\{ \frac{1}{(s+k)^4} + \frac{1}{(1-s+k)^4} \right\} & j = 2, \ldots, N_B \end{cases}$$

where $s=(j-1)/N$ and piecewise linear basis function have been used for approximating both, u and λ. For interior circular domains the eigenvalues λ_{V_i} and λ_{D_i} $(i \in \mathcal{I}_B \setminus \{p\})$ coincide with those mentioned above, whereas the eigenvalues of $\tilde{K}_i := K_i + \frac{1}{2} I_i$ become different

$$\lambda_{\tilde{K}_i, j} = \begin{cases} 0 & j=1 \\ \frac{1}{2}h\left(\frac{\sin \pi s}{\pi}\right)^4 \sum_{k=0}^{\infty} \left\{ \frac{1}{(s+k)^4} + \frac{1}{(1-s+k)^4} \right\} & j=2,\ldots, N_B. \end{cases}$$

6. Parallel Solution

6.1 Transformation and Spectral Equivalence Results

The nonsymmetric, positive definite system (18) can be approximately solved by Bramble/Pasciak's CG method [1]. The method requires a preconditioner C_Λ which can be inverted easily and which fulfills the spectral equivalence inequalities

$$\underline{\gamma}_\Lambda C_\Lambda \leq K_\Lambda \leq \overline{\gamma}_\Lambda C_\Lambda, \quad \text{with} \quad \underline{\gamma}_\Lambda > 1. \tag{20}$$

With the definitions

$$K_1 = K_\Lambda, \mathbf{f}_1 = \mathbf{f}_\Lambda$$

$$K_{12} = K_{21}^T = (-K_{\Lambda C}\ 0)$$

$$K_2 = \begin{pmatrix} K_C & K_{CI} \\ K_{IC} & K_I \end{pmatrix}, \quad \mathbf{f}_2 = \begin{pmatrix} -\mathbf{f}_C \\ -\mathbf{f}_I \end{pmatrix}$$

we can reformulate (18) as a symmetric but indefinite system:

$$\begin{pmatrix} K_1 & K_{12} \\ K_{21} & -K_2 \end{pmatrix} \begin{pmatrix} \mathbf{u}_1 \\ \mathbf{u}_2 \end{pmatrix} = \begin{pmatrix} \mathbf{f}_1 \\ \mathbf{f}_2 \end{pmatrix}. \tag{21}$$

Following Bramble and Pasciak [1] this system can be transformed into

$$G\mathbf{u} = \mathbf{p}, \tag{22}$$

where

$$G := \begin{pmatrix} C_\Lambda^{-1} K_1 & C_\Lambda^{-1} K_{12} \\ K_{21} C_\Lambda^{-1}(K_1 - C_\Lambda) & K_2 + K_{21} C_\Lambda^{-1} K_{12} \end{pmatrix}$$

and

$$\mathbf{p} = \begin{pmatrix} C_\Lambda^{-1} \mathbf{f}_1 \\ K_{21} C_\Lambda^{-1} \mathbf{f}_1 - \mathbf{f}_2 \end{pmatrix}.$$

Then, the matrix G is self-adjoint and positive definite with respect to the scalar product $[.;.]$ which is defined by

$$[\mathbf{w}, \mathbf{v}] := ((K_1 - C_\Lambda)\mathbf{w}_1, \mathbf{v}_1) + (\mathbf{w}_2, \mathbf{v}_2). \tag{23}$$

Moreover, G is spectrally equivalent to the regularisator R, where

$$R := \begin{pmatrix} I & 0 \\ 0 & K_2 + K_{21}K_1^{-1}K_{12} \end{pmatrix}.$$

Bramble and Pasciak [1] proved the spectral equivalence inequalities

$$\underline{\lambda}[R\mathbf{v}, \mathbf{v}] \leq [G\mathbf{v}, \mathbf{v}] \leq \bar{\lambda}[R\mathbf{v}, \mathbf{v}] \quad \forall \mathbf{v} \in \mathbf{R}^N, \tag{24}$$

where

$$\underline{\lambda} = \left(1 + \frac{\alpha}{2} + \sqrt{\alpha + \frac{\alpha^2}{4}}\right)^{-1} \quad \text{and} \quad \bar{\lambda} = \frac{1 + \sqrt{\alpha}}{1 - \alpha} \tag{25}$$

with $\alpha = 1 - (1/\bar{\gamma}_\Lambda)$. Thus, we have to find a preconditioner C_2 for the matrix

$$K_2 + K_{21}K_1^{-1}K_{12} = \begin{pmatrix} K_C + K_{C\Lambda}K_\Lambda^{-1}K_{\Lambda C} & K_{CI} \\ K_{IC} & K_I \end{pmatrix}. \tag{26}$$

The DD preconditioner defined by

$$C_2 = \begin{pmatrix} I_C & K_{CI}B_I^{-T} \\ 0 & I_I \end{pmatrix} \begin{pmatrix} C_C & 0 \\ 0 & C_I \end{pmatrix} \begin{pmatrix} I_C & 0 \\ B_I^{-1}K_{IC} & I_I \end{pmatrix} \tag{27}$$

is spectrally equivalent to $K_2 + K_{21}K_1^{-1}K_{12}$ if we have preconditioners C_I and C_C fulfilling the inequalities

$$\underline{\gamma}_C C_C \leq \tilde{S}_C + K_{C\Lambda}K_\Lambda^{-1}K_{\Lambda C} \leq \bar{\gamma}_C C_C, \tag{28}$$

$$\underline{\gamma}_I C_I \leq K_I \leq \bar{\gamma}_I C_I, \tag{29}$$

where

$$\tilde{S}_C = K_C - K_{CI}K_I^{-1}K_{IC} + K_{CI}\left(K_I^{-1} - B_I^{-T}\right)K_I\left(K_I^{-1} - B_I^{-1}\right)K_{IC}.$$

The following lemma holds [30, 31].

Lemma 1. *If the symmetric and positive definite block preconditioners* $C_I = diag(C_{I,i})_{i \in \mathcal{I}_F}$ *and* C_C *satisfy the spectral equivalence inequalities* (28) *and* (29) *with positive constants* $\underline{\gamma}_C$, $\bar{\gamma}_C$, $\underline{\gamma}_I$, $\bar{\gamma}_I$, *then the spectral equivalence inequalities*

$$\underline{\gamma}_2 C_2 \leq K_2 + K_{21}K_1^{-1}K_{12} \leq \bar{\gamma}_2 C_2 \tag{30}$$

hold for the preconditioner C_2 *defined by* (27) *with the constants*

$$\underline{\gamma}_2 = \min\{\underline{\gamma}_C, \underline{\gamma}_I\}\left(1 - \sqrt{\frac{\mu}{1+\mu}}\right) \quad \text{and} \quad \bar{\gamma}_2 = \max\{\bar{\gamma}_C, \bar{\gamma}_I\}\left(1 + \sqrt{\frac{\mu}{1+\mu}}\right). \tag{31}$$

Here $\mu = \rho(S_C^{-1} T_C)$ *denotes the spectral radius of* $S_C^{-1} T_C$, *with* $S_C = \mathring{K}_C - \mathring{K}_{CI} K_I^{-1} \mathring{K}_{IC}$ *denoting the f.e. Schur complement, and* $T_C = \mathring{K}_{CI}(K_I^{-1} - B_I^{-T}) K_I (K_I^{-1} - B_I^{-1}) \mathring{K}_{IC}$.

The proof is given in [30], it applies the classical f.e. DD spectral equivalence result proved in [13]. With (25) we conclude the following theorem.

Theorem 1. *If the conditions imposed on* C_A, C_C, C_I, *and* B_I, *especially* (20), (28), *and* (29) *are satisfied, then the f.e./b.e. DD preconditioner*

$$C = \operatorname{diag}(I_1, C_2) \tag{32}$$

is self-adjoint and positive definite with respect to the inner product [.,.] *and satisfies the spectral equivalence inequalities*

$$\underline{\gamma}[C\mathbf{v}, \mathbf{v}] \leq [G\mathbf{v}, \mathbf{v}] \leq \bar{\gamma}[C\mathbf{v}, \mathbf{v}] \quad \forall \mathbf{v} \in \mathbf{R}^N, \tag{33}$$

with the constants

$$\underline{\gamma} = \underline{\lambda} \min\{1, \underline{\gamma}_2\} \quad \text{and} \quad \bar{\gamma} = \bar{\lambda} \max\{1, \bar{\gamma}_2\},$$

where $\underline{\lambda}$, $\bar{\lambda}$, $\underline{\gamma}_2$, $\bar{\gamma}_2$ *are given in* (25) *and* (31), *respectively.*

6.2 The Parallel PCG Algorithm

For the vectors belonging to the inner coupling boundary Γ_C we define two types of distribution called overlapping (type 1) and adding (type 2):

type 1: $\mathbf{u}_C, \mathbf{w}_C, \mathbf{s}_C$ are stored in P_i as $\mathbf{u}_{C,i} = A_{C,i}\mathbf{u}_C$, $\mathbf{w}_{C,i} = A_{C,i}\mathbf{w}_C$, $\mathbf{s}_{C,i} = A_{C,i}\mathbf{s}_C$

type 2: $\mathbf{r}_C, \mathbf{v}_C, \mathbf{f}_C$ are stored in P_i as $\mathbf{r}_{C,i}, \mathbf{v}_{C,i}, \mathbf{f}_{C,i}$ such that

$\mathbf{r}_C = \sum_{i=1}^{p} A_{C,i}^T \mathbf{r}_{C,i}$ etc.,

where the matrices $A_{C,i}$ are the "C-block" of the Boolean subdomain connectivity matrix A_i which maps some overall vector of parameters associated with the subdomain $\bar{\Omega}_i$ only.

Using this notation and the operators introduced in the previous section we can formulate an improved version of the PCG-algorithm presented in [30] with a given accuracy ϵ as stopping criterion.

Note the vectors $\mathbf{z}_i = (\mathbf{z}_{A,i}, \mathbf{z}_{C,i}, \mathbf{z}_{AC,i})^T$ and $\mathbf{h}_i = (\mathbf{h}_{A,i}, \mathbf{h}_{C,i}, \mathbf{h}_{AC,i})^T$ which have been inserted additionally in order to achieve a synchronization between the FEM and BEM processors especially in step 1 (matrix-times-vector operation). Without this synchronization one has to expect a computation time per iteration which is, depending on the problem, up to 30 per cent higher. The definition of the vector $\mathbf{p}_i$ avoids the computation of $C_{A,i}\mathbf{r}_{A,i}$ (occurred originally in step 4) which is not necessarily available ($C_{A,i}$ is defined such that the inverse operation $C_{A,i}^{-1}\mathbf{w}_{A,i}$ can be performed easily).

	FEM ($i \in \mathcal{I}_F$)	BEM ($i \in \mathcal{I}_B$)
0.	Starting step	
	Choose an initial guess $\mathbf{u} = \mathbf{u}_0$	
	$\mathbf{u}_i = \begin{bmatrix} \mathbf{u}_{C,i} \\ \mathbf{u}_{I,i} \end{bmatrix}$	$\mathbf{u}_i = \begin{bmatrix} \mathbf{u}_{\Lambda,i} \\ \mathbf{u}_{C,i} \end{bmatrix}$
	$\mathbf{r}_{I,i} = \mathbf{f}_{I,i} - K_{IC,i}\mathbf{u}_{C,i} - K_{I,i}\mathbf{u}_{I,i}$ $\mathbf{r}_{C,i} = \mathbf{f}_{C,i} - K_{C,i}\mathbf{u}_{C,i} - K_{CI,i}\mathbf{u}_{I,i}$	$\mathbf{v}_{\Lambda,i} = \mathbf{f}_{\Lambda,i} - K_{\Lambda,i}\mathbf{u}_{\Lambda,i} + K_{\Lambda C,i}\mathbf{u}_{C,i}$ $\mathbf{r}_{\Lambda,i} = C_{\Lambda,i}^{-1}\mathbf{v}_{\Lambda,i}$ $\mathbf{r}_{C,i} = \mathbf{f}_{C,i} - K_{C,i}\mathbf{u}_{C,i} - K_{C\Lambda,i}\mathbf{u}_{\Lambda,i}$ $\mathbf{r}_{C,i} = \mathbf{r}_{C,i} - K_{C\Lambda,i}\mathbf{r}_{\Lambda,i}$
	$\mathbf{v}_{C,i} = \mathbf{r}_{C,i} - K_{CI,i}B_{I,i}^{-T}\mathbf{r}_{I,i}$	$\mathbf{w}_{\Lambda,i} = \mathbf{r}_{\Lambda,i}, \quad \mathbf{p}_i = \mathbf{v}_{\Lambda,i}$ $\mathbf{v}_{C,i} = \mathbf{r}_{C,i}, \quad \mathbf{z}_{\Lambda,i} = K_{\Lambda,i}\mathbf{w}_{\Lambda,i}$
	$\mathbf{w}_{C,i} = A_{C,i}\mathbf{w}_C \leftarrow \mathbf{w}_C = C_C^{-1}\sum_{i=1}^{p} A_{C,i}^T\mathbf{v}_{C,i} \rightarrow \mathbf{w}_{C,i} = A_{C,i}\mathbf{w}_C$	
	$\mathbf{w}_{I,i} = C_{I,i}^{-1}\mathbf{r}_{I,i} - B_{I,i}^{-1}K_{IC,i}\mathbf{w}_{C,i}$	$\mathbf{z}_{\Lambda C,i} = K_{\Lambda C,i}\mathbf{w}_{C,i}, \quad \mathbf{z}_{C,i} = K_{C,i}\mathbf{w}_{C,i}$
	$\mathbf{s} = \mathbf{w}$	$\mathbf{s} = \mathbf{w}$
	$\sigma_i = \mathbf{r}_{C,i}^T\mathbf{w}_{C,i} + \mathbf{r}_{I,i}^T\mathbf{w}_{I,i}$	$\sigma_i = \mathbf{r}_{C,i}^T\mathbf{w}_{C,i} + \mathbf{w}_{\Lambda,i}^T(\mathbf{z}_{\Lambda,i} - \mathbf{p}_i)$
	$\sigma = \sigma^0 = \sum_{i=1}^{p}\sigma_i$	
	Iteration	
1.	$\mathbf{v}_{I,i} = K_{IC,i}\mathbf{s}_{C,i} + K_{I,i}\mathbf{s}_{I,i}$ $\mathbf{v}_{C,i} = K_{C,i}\mathbf{s}_{C,i} + K_{CI,i}\mathbf{s}_{I,i}$ $\delta_i = \mathbf{v}_C^T\mathbf{s}_C + \mathbf{v}_{I,i}^T\mathbf{s}_{I,i}$	$\mathbf{w}_{\Lambda,i} = \mathbf{z}_{\Lambda,i} - \mathbf{z}_{\Lambda C,i}$ $\mathbf{v}_{\Lambda,i} = C_{\Lambda,i}^{-1}\mathbf{w}_{\Lambda,i}$ $\mathbf{v}_{C,i} = \mathbf{z}_{C,i} + K_{C\Lambda,i}(\mathbf{s}_{\Lambda,i} - \mathbf{v}_{\Lambda,i})$ $\delta_i = \mathbf{v}_{C,i}^T\mathbf{s}_{C,i} + \mathbf{v}_{\Lambda,i}^T\mathbf{z}_{\Lambda,i} - \mathbf{w}_{\Lambda,i}^T\mathbf{s}_{\Lambda,i}$
	$\delta = \sum_{i=1}^{p}\delta_i$	
	$\alpha = \sigma/\delta$	$\alpha = \sigma/\delta$
2.	$\hat{\mathbf{u}}_i = \mathbf{u}_i + \alpha\mathbf{s}_i$ $\hat{\mathbf{r}}_i = \mathbf{r}_i - \alpha\mathbf{v}_i$	$\hat{\mathbf{u}}_i = \mathbf{u}_i + \alpha\mathbf{s}_i$ $\hat{\mathbf{r}}_i = \mathbf{r}_i - \alpha\mathbf{v}_i$
3.	$\hat{\mathbf{v}}_{C,i} = \hat{\mathbf{r}}_{C,i} - K_{CI,i}B_{I,i}^{-T}\hat{\mathbf{r}}_{I,i}$	$\hat{\mathbf{v}}_{C,i} = \hat{\mathbf{r}}_{C,i}, \quad \mathbf{h}_{\Lambda,i} = K_{\Lambda,i}\hat{\mathbf{r}}_{\Lambda,i}$
	$\mathbf{w}_{C,i} = A_{C,i}\mathbf{w}_C \leftarrow \mathbf{w}_C = C_C^{-1}\sum_{i=1}^{p} A_{C,i}^T\mathbf{v}_{C,i} \rightarrow \mathbf{w}_{C,i} = A_{C,i}\mathbf{w}_C$	
	$\hat{\mathbf{w}}_{I,i} = C_{I,i}^{-1}\hat{\mathbf{r}}_{I,i} - B_{I,i}^{-1}K_{IC,i}\hat{\mathbf{w}}_{C,i}$	$\hat{\mathbf{w}}_{\Lambda,i} = \hat{\mathbf{r}}_{\Lambda,i}, \quad \hat{\mathbf{p}}_i = \mathbf{p}_i - \alpha\mathbf{w}_{\Lambda,i}$ $\mathbf{h}_{\Lambda C,i} = K_{\Lambda C,i}\hat{\mathbf{w}}_{C,i}$ $\mathbf{h}_{C,i} = K_{C,i}\hat{\mathbf{w}}_{C,i}$
4.	$\sigma_i = \hat{\mathbf{r}}_{C,i}^T\hat{\mathbf{w}}_{C,i} + \hat{\mathbf{r}}_{I,i}^T\hat{\mathbf{w}}_{I,i}$	$\sigma_i = \hat{\mathbf{r}}_{C,i}^T\hat{\mathbf{w}}_{C,i} + \mathbf{h}_{\Lambda,i}^T\hat{\mathbf{r}}_{\Lambda,i} - \hat{\mathbf{p}}_i^T\hat{\mathbf{r}}_{\Lambda,i}$
	$\hat{\sigma} = \sum_{i=1}^{p}\sigma_i$	
	$\beta = \hat{\sigma}/\sigma$	$\beta = \hat{\sigma}/\sigma$
5.	$\hat{\mathbf{s}}_i = \hat{\mathbf{w}}_i + \beta\mathbf{s}_i$	$\hat{\mathbf{s}}_i = \hat{\mathbf{w}}_i + \beta\mathbf{s}_i, \quad \hat{\mathbf{z}}_i = \mathbf{h}_i + \beta\mathbf{z}_i$
6.	If $\hat{\sigma} \leq \varepsilon^2 * \sigma^0$, then STOP else goto step 1.	

7. Nonlinear Problems

As an application, let us consider a class of nonlinear magnetic field problems. In many cases, the linear model is not sufficient for modelling electromagnetic phenomena. Therefore we take into account that for ferromagnetic materials the permeability depends on the absolute value of the magnetic induction, i.e. there is a material function $\nu(|\mathrm{B}|) = \nu(|\nabla u|)$ with

$$\mathrm{H} = \nu(|\mathrm{B}|)\mathrm{B},$$

where H is the magnetic field strength. Formally the problem can be written as

$$\begin{aligned} -\operatorname{div}\left(\nu(x, |\nabla u(x)|)\,\nabla u(x)\right) &= \mathrm{S}(x) + \frac{\partial \mathrm{H}_{0y}(x)}{\partial \mathrm{x}} - \frac{\partial \mathrm{H}_{0x}(x)}{\partial \mathrm{y}}, \quad x \in \Omega \\ u(x) &= 0,\ x \in \Gamma_D \\ |u(x)| &\to 0 \text{ for } |x| \to \infty. \end{aligned} \tag{34}$$

The analysis of nonlinear magnetic field problems (in bounded domains) can be found in [20–24]. The solution of these problems using multigrid-Newton methods is examined in [21, 23]. There, numerical results for practical problems are documented, too.

Here, we allow ferromagnetic materials with non-constant permeability ν to be in the f.e. subdomains only. Hence, the discretization results in a nonlinear system [25, 27]

$$K\begin{pmatrix} \mathbf{u}_\Lambda \\ \mathbf{u}_C \\ \mathbf{u}_I \end{pmatrix} = K_F\begin{pmatrix} \mathbf{u}_C \\ \mathbf{u}_I \end{pmatrix} + K_B \cdot \begin{pmatrix} \mathbf{u}_\Lambda \\ \mathbf{u}_C \end{pmatrix} = \begin{pmatrix} \mathbf{f}_\Lambda \\ \mathbf{f}_C \\ \mathbf{f}_I \end{pmatrix}, \tag{35}$$

where the nonlinear operator $K{:}\mathbf{R}^N \to \mathbf{R}^N$ can be split up into the nonlinear operator $K_F{:}\mathbf{R}^{N_C+N_I} \to \mathbf{R}^N$ originating from the nonlinear form

$$a_{FN}(u, v) := \sum_{i \in \mathscr{T}_F} \int_{\Omega_i} \nu(x, |\nabla u|)\, \nabla^{\top} u(x)\, \nabla v(x)\, dx$$

and the linear operator $K_B{:}\mathbf{R}^{N_\Lambda+N_C} \to \mathbf{R}^N$ originating from a_B [25, 27]. The nonlinear system (35) is solved by Newton's method, cf. [25, 27].

Then, the linear Newton defect system with the Jacobi matrix $K'[\mathbf{u}]$ is given by

$$K'\left[\begin{pmatrix} \mathbf{u}_\Lambda \\ \mathbf{u}_C \\ \mathbf{u}_I \end{pmatrix}\right] \cdot \begin{pmatrix} \mathbf{w}_\Lambda \\ \mathbf{w}_C \\ \mathbf{w}_I \end{pmatrix} = K_F'\left[\begin{pmatrix} \mathbf{u}_C \\ \mathbf{u}_I \end{pmatrix}\right] \cdot \begin{pmatrix} \mathbf{w}_C \\ \mathbf{w}_I \end{pmatrix} + K_B \cdot \begin{pmatrix} \mathbf{w}_\Lambda \\ \mathbf{w}_C \end{pmatrix} = \begin{pmatrix} \mathbf{d}_\Lambda \\ \mathbf{d}_C \\ \mathbf{d}_I \end{pmatrix}. \tag{36}$$

It can be rewritten in a block form similar to (18),

$$\begin{pmatrix} K_\Lambda & -K_{\Lambda C} & 0 \\ K_{C\Lambda} & K_C & K_{CI} \\ 0 & K_{IC} & K_I \end{pmatrix} \begin{pmatrix} \mathbf{w}_\Lambda \\ \mathbf{w}_C \\ \mathbf{w}_I \end{pmatrix} = \begin{pmatrix} \mathbf{d}_\Lambda \\ \mathbf{d}_C \\ \mathbf{d}_I \end{pmatrix}, \tag{37}$$

and can be solved by a PCG method as described in Section 6.

Further, we apply the "nested iteration" method [16, 23]. We generate a multilevel sequence of coupled f.e./b.e. discretizations denoted by the grid numbers $q = 1, \ldots, l$. We begin with solving the nonlinear system by Newton's method on the coarsest grid $q = 1$. Then we take the approximate solution on the grid $q - 1$ interpolated onto the finer grid q as an initial approximation for Newton's method on the grid q, for $q = 2, \ldots, l$. This allows us to "catch" the nonlinearity on the coarsest grid, cf. [23].

The parallel nested Newton algorithm is described in detail in [25–27]. From a practical point of view more interesting applications are described in [25, 27].

8. Applications

8.1 Far Field Computations

If values of $u(.)$ or even of the derivative $\dfrac{\partial u(.)}{\partial x}$ are required for points $x \in \Omega_+$ we can use the following representation formulae

$$u(x) = \int_{\Gamma_+} \left(u(y) \frac{\partial}{\partial n_y} E(x, y) - E(x, y) \frac{\partial}{\partial n_y} u(y) \right) ds_y, \tag{38}$$

$$\frac{\partial u(x)}{\partial x} = \int_{\Gamma_+} \left(u(y) \frac{\partial^2}{\partial n_y \partial x} E(x, y) - \frac{\partial}{\partial x} E(x, y) \frac{\partial}{\partial n_y} u(y) \right) ds_y. \tag{39}$$

Note, in opposite to the FEM we are able to compute the derivative of u directly and without any loss of accuracy. The integrals can be computed numerically using the basis functions ϕ_j, $j = N_\Lambda - N_{\Lambda,p} + 1, \ldots, N_\Lambda$, introduced above which are in our case piecewise linear. Then we obtain an approximation $\tilde{u}(x)$ for $u(x)$ $(x \in \Omega_+)$ from (38)

$$\tilde{u}(x) = \sum_{i,j=N_\Lambda - N_{\Lambda,p}+1}^{N_\Lambda} \left(\frac{\partial}{\partial n_y} E(x, y_i) u(y_j) - E(x, y_j) \frac{\partial}{\partial n_y} u(y_i) \right) \int_{\Gamma_+} \phi_i(y) \phi_j(y)$$

$$= \mathbf{E}_{\Lambda,p}(x)^T M_p \mathbf{u}_p - \mathbf{u}_{\Lambda,p}^T M_p \mathbf{E}_p(x), \tag{40}$$

where $\mathbf{E}_p(x) := [E(x, y_{N_\Lambda - N_{\Lambda,p}+1}), \ldots, E(x, y_{N_\Lambda})]^T$ and

$$\mathbf{E}_{\Lambda,p}(x) := \left[\frac{\partial}{\partial n_y} E(x, y_{N_\Lambda - N_{\Lambda,p}+1}), \ldots, \frac{\partial}{\partial n_y} E(x, y_{N_\Lambda}) \right]^T,$$

and M_p is the mass matrix with the elements

$$m_{ij,p} := \int_{\Gamma_+} \phi_i(y) \phi_j(y) \, ds_y, \quad i, j = N_\Lambda - N_{\Lambda,p} + 1, \ldots, N_\Lambda.$$

In the same way we obtain a numerical approximation $\tilde{u}_x(x)$ of the gradient of $u(x)$ for $x \in \Omega_+$:

$$\tilde{u}_x(x) = \mathbf{E}_{\Lambda x,p}(x)^T M_p \mathbf{u}_p - u_{\Lambda,p}^T M_p \mathbf{E}_{x,p}(x), \tag{41}$$

where

$$\mathbf{E}_{\Lambda x,p}(x) := \left[\frac{\partial^2}{\partial n_y \partial x} E(x, y_{N_\Lambda - N_{\Lambda,p}+1}), \ldots, \frac{\partial^2}{\partial n_y \partial x} E(x, y_{N_\Lambda}) \right]^T$$

$$\mathbf{E}_{x,p}(x) := \left[\frac{\partial}{\partial x} E(x, y_{N_\Lambda - N_{\Lambda,p}+1}), \ldots, \frac{\partial}{\partial x} E(x, y_{N_\Lambda}) \right]^T.$$

Summarizing we can give the following table for approximating values of u and of the derivative of u for both, exterior and interior domains, the latter after analogous considerations and appropriate definitions of $\mathbf{E}_i$, $\mathbf{E}_{\Lambda,i}$, $\mathbf{E}_{x,p}$, $\mathbf{E}_{\Lambda x,\mathrm{p}}$ $(i \in \mathcal{I}_B \setminus \{p\})$.

exterior domain	interior domain $(i \in \mathcal{I}_B \setminus \{p\})$
$\tilde{u}(x) = \mathbf{E}_{\Lambda,p}(x)^T M_p \mathbf{u}_p - \mathbf{u}_{\Lambda,p}^T M_p \mathbf{E}_p(x)$	$\tilde{u}(x) = -\mathbf{E}_{\Lambda,i}(x)^T M_i \mathbf{u}_i + \mathbf{u}_{\Lambda,i}^T M_i \mathbf{E}_i(x)$
$\tilde{u}_x(x) = \mathbf{E}_{\Lambda x,p}(x)^T M_p \mathbf{u}_p - \mathbf{u}_{\Lambda,p}^T M_p \mathbf{E}_{x,p}(x)$	$\tilde{u}_x(x) = -\mathbf{E}_{\Lambda x,i}(x)^T M_i \mathbf{u}_i + \mathbf{u}_{\Lambda,i}^T M_i \mathbf{E}_{x,i}(x)$

8.2 The Implementation

The algorithm is implemented in the parallel code FEM⊂⊃BEM [10] and has been tested on a parallel system GC Power Plus using 32 processors (Example 1) and on a Power Xplorer using 8/4 processors (Example 2). The components of the algorithm are chosen in the following way:

C_I: multigrid V02 (Example 1) and V11 (Example 2) cycle in the symmetric Multiplicative Schwarz Method [12, 13];
B_I: implicitly defined by hierarchical extension (formally $E_{IC} = -B_I^{-1} K_{IC}$) [15];
C_C: applying a Bramble/Pasciak/Xu [34, 3] type preconditioner (BPX), for the preconditioning of the cross-point system (cf. [13]) an artificial boundary is introduced;
C_Λ: scaled single layer potential b.e. matrix for circular domain which is a circulant [32] (Circ), or properly scaled preconditioner as described in [33] by Steinbach based on the BEM mass matrix and the hypersingular operator (Hyper).

These preconditioners C_I, C_C, C_Λ, and the basis transformation B_I satisfy the conditions stated in Theorem 1. In particular, inequalities (29) for C_I are fulfilled with constants $\underline{\gamma}_I$, $\overline{\gamma}_I$ independent of the discretization parameter h. We refer to [13] and [12, 15] for the application of the symmetric Multiplicative Schwarz Method and its interpretation as an Additive Schwarz Method. The preconditioner C_Λ is scaled such that the constant $\overline{\gamma}_\Lambda$ in (20), (25) is independent of h for both, (Circ) and (Hyper), cf. [33].

Further, the constant μ in (31) can be estimated by $\mu \leq \eta^{2k}(1 + c_1 l)^2 \leq \eta^{2k}(1 + c_2(\ln h^{-1}))^2$, cf. [15], with k being the number of local multigrid iterations, l being the number of grids, the h-independent multigrid rate $\eta < 1$, and the h-independent constants c_i. Thus, μ is independent of h if $k = \mathcal{O}(\ln \ln h^{-1})$.

The inequalities in (28) hold with an h-independent constant $\underline{\gamma}_C$, and $\bar{\gamma}_C \leq c_3(1 + \mu)$, cf. [15, 34].

Therefore, we can prove that $\bar{\gamma}/\underline{\gamma} \leq c_4(1 + \mu)(\sqrt{\mu} + \sqrt{1 + \mu})^2 = \mathcal{O}(1)$ if $k = \mathcal{O}(\ln \ln h^{-1})$. However, in practice, $k = 1$ gives the minimal computing time even if the number of CG iterations grows moderate, cf. Table 1.

Table 1. Performance of the algorithm (Example 1) on a GC Power Plus ($\epsilon = 10^{-6}$)

Grid	No. of unknowns	No. of CG iterations	Overall time (sec)
1	573	15	1.9
2	2184	20	3.0
3	8556	21	3.6
4	33900	22	6.0
5	134988	23	14.0
6	538764	24	45.6

8.3 A Linear Problem

In our first example we simulate an electrical device consisting of six permanent magnets as shown in Fig. 1. The structure is symmetric, in particular each sector of iron encloses an angle of 24° and, consequently, each magnet encloses an

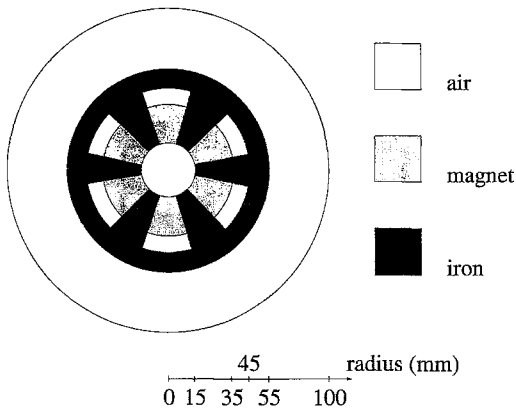

Figure 1. Cross section of the device

angle of 36°. The magnets do have a magnetization of 1 Tesla and they are polarized alternately. The material dependent coefficients are defined by

$$\nu_{magnet} = 750000.0\ \mathrm{AmV^{-1}s^{-1}},$$
$$\nu_{air} = 795774.4\ \mathrm{AmV^{-1}s^{-1}},$$
$$\nu_{iron} = 1000.0\ \mathrm{AmV^{-1}s^{-1}},$$

that is we are given a linear problem.

The interior domain has been divided into 31 subdomains, so that altogether 32 processors are required. The picture on the left in Fig. 2 shows the equipotential lines of the vector potential within the interior domain. Most of the potential lines are lying inside the iron coating, the ones going outside indicate change of polarization.

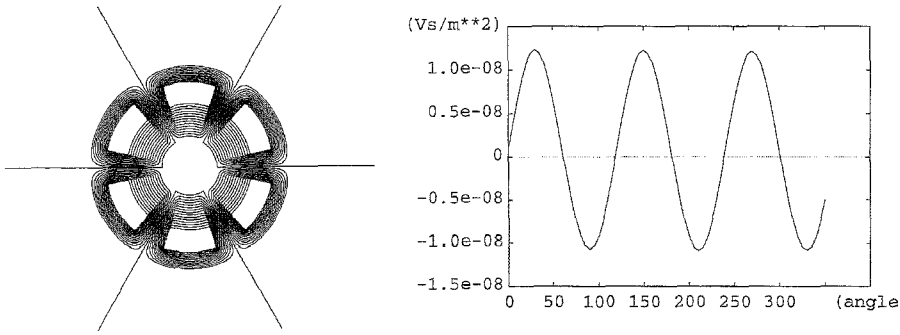

Figure 2. Equipotential lines and far field results for Example 1

Now we are interested in the far field behaviour of the magnetic field. For this purpose we have computed the tangential component of the magnetic induction along the circle with the radius $r = 1\mathrm{m}$ (see picture on the right in Fig. 2).

Finally we want to give a table showing the performance of the algorithm (Table 1).

8.4 The Electromagnet

In the second example we want to compute the magnetic induction caused by an electromagnet as it is shown in Fig. 3. The copper domains, where we assume to be a current density of the strength S, and the iron domain, are squares with the edges being 16cm long. The material dependent coefficients are defined by

$$\nu_{copper} = 795779.0\ \mathrm{AmV^{-1}s^{-1}},$$
$$\nu_{air} = 795774.4\ \mathrm{AmV^{-1}s^{-1}}.$$

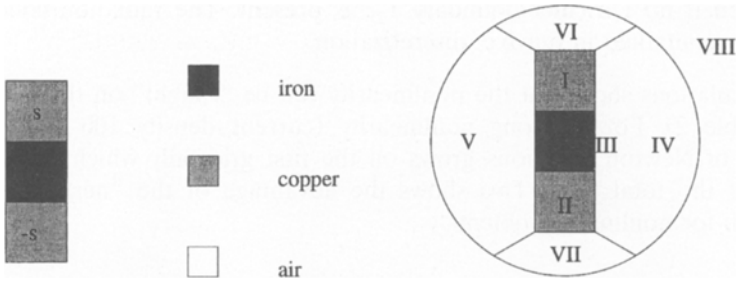

Figure 3. The magnet and the subdomains being used

The coefficient ν_{iron} of the ferromagnetic material is assumed to be dependent on the induction B, that is we are faced with a nonlinear problem now. In our application, discrete values of ν_{iron} are given and a special interpolation technique, which maintains monotonicity, for approximating ν_{iron} at arbitrary points is applied, cf. [24].

We will compare two different coupling procedures. On the one hand we use the natural boundary (of the metallic material) as coupling boundary and on the other hand we introduce a circle with the radius 50cm as coupling boundary. The advantage of the second method is that we obtain circulant matrices which can be generated very fast whereas the first method requires the generation of fully populated matrices. A disadvantage of the second method is that additional subdomains and, thus, additional unknowns have to be introduced. For the second method, the f.e. mesh of the first grid is shown in Fig. 4. Finer grids are obtained by an uniform refinement, that is by dividing each triangle into four congruent subtriangles. Numerical results are given in Table 2, the slash (/) marks the change of the accuracy in the CG-solver from 10^{-2} to 10^{-4}. For this example, the uniqueness of the solution is guaranteed by the radiation condi-

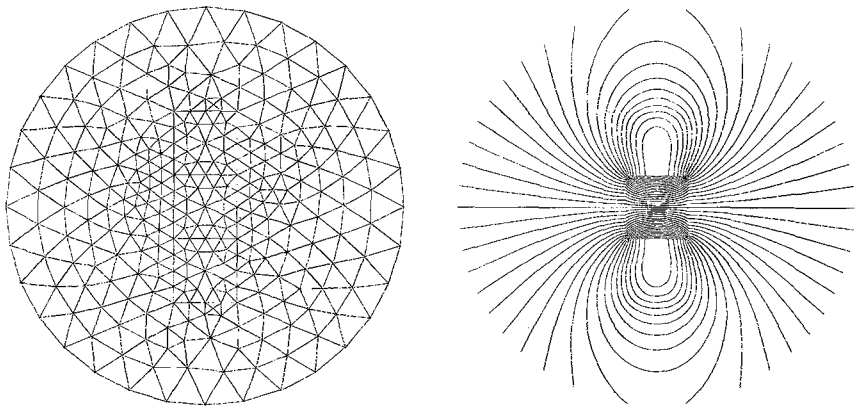

Figure 4. The mesh (1st grid) being used and the equipotential lines of A (Example 2: electric magnet).

tion, even if no Dirichlet boundary Γ_D is present. The radiation condition is implicitly contained in our b.e. discretization.

The calculations show that the nonlinearity can be "caught" on the coarse grid (see Table 2). For a strong nonlinearity (current density 100 A/mm^2) the number of Newton iterations grows on the first grid only which takes a little quota of the total time. This shows the advantage of the "nested iteration" approach for nonlinear problems.

Table 2. Calculations for Example 2 (electromagnet, whole $\mathbf{R}^2$)

Current density (A/mm^2)	1	100	1	100	1	100
Shape of Γ_+	circle				rectangle	
subdomains (processors)	FEM: I-VII BEM: VIII		FEM: I-III BEM: IV-VIII		FEM: I-III BEM: exterior	
Number of unknowns	68353		18429		16129	
Choice for C_Λ	Circ		Circ + Hyper		Hyper	
Newton iterations 1st grid	3	9	3	9	3	9
Newton iterations 2nd grid	2	2	2	2	2	2
CG iterations 2nd grid	6,7	5,7	7,8	7,8	6,7	6,7
Newton iterations 3rd grid	2	2	2	2	2	2
CG iterations 3rd grid	6,7	6,7	8,8	8,8	6,8	6,8
Newton iterations 4th grid	2	2	2	2	2	3
CG iterations 4th grid	6,8	6,8	8,8	8,8	7,8	7,8
Newton iterations 5th grid	3	3	3	3	3	3
CG iterations 5th grid	6,9/16	7,9/16	7,8/16	7,9/17	7,8/14	7,9/18
Time (system generation)	12.3	13.2	15.6	16.7	18.7	19.1
Time (linear solver)	35.4	39.2	19.5	22.0	18.0	19.2
Total time	48.5	53.2	35.9	39.5	37.5	39.1

Time in seconds, Power Xplorer; $\varepsilon = 10^{-6}$

Comparing the three choices of the subdomains and their discretization, we observe that in the first choice (columns 1/2) much time is spent for handling the FEM subdomains IV, V with many interior nodes. We may conclude that the BEM (columns 3/4) is recommended for subdomains with a high ratio between the numbers of interior FEM nodes and the boundary nodes. The choice of the rectangular coupling boundary (columns 5/6) increases the BEM system generation effort, but the total time remains nearly the same since the number of BEM unknowns (and subdomains) is reduced.

9. Concluding Remarks

The aim of this paper was to marry the advantages of FEM and BEM and to present an efficient parallel algorithm for solving linear and nonlinear exterior problems. The DD-method turned out to be a good basis for the coupling of the

two methods. The full Galerkin scheme (FEM and BEM) and some transformation gave rise to a positive definite self-adjoint system which has been solved by the parallel PCG-algorithm. The numerical results given in the previous section show that different coupling techniques are admissible and all of them lead to satisfying computation times. Although we had started off using BEM in order to model exterior problems correctly, we have also demonstrated that the use of boundary elements is not restricted to the exterior domain. At the end, the right choice of the discretization method for each subdomain and, first of all, the definition of the subdomains themselves (including the coupling boundary Γ_+) depends on the actual problem which is to be solved.

References

[1] Bramble, J. H., Pasciak, J. E.: A preconditioning technique for indefinite systems resulting from mixed approximation of elliptic problems. Math. Comput. *50*, 1–17 (1988).

[2] Bramble, J. H., Pasciak, J. E., Schatz, A. H.: The construction of preconditioners for elliptic problems by substructuring I-IV. Math. Comput. *47*, 103–134 (1986); *49*, 1–16 (1987); *51*, 415–430 (1988); *53*, 1–24 (1989).

[3] Bramble, J. H., Pasciak, J. E., Xu, J.: Parallel multilevel preconditioners. Math. Comput. *55*, 1–22 (1990).

[4] Chan, T. F., Glowinski, R., Periaux, J., Widlund, O. B.: Domain decomposition methods for partial differential equations. Proc. of the 2nd International Symposium, Los Angeles, 1988. Philadelphia: SIAM 1989.

[5] Chan, T. F., Glowinski, R., Periaux, J., Widlund, O. B.: Domain decomposition methods for partial differential equations. Proc. of the 3rd International Symposium, Houston, 1989. Philadelphia: SIAM 1990.

[6] Costabel, M.: Symmetric methods for the coupling of finite elements and boundary elements. In: Boundary elements IX, (Brebbia, C. A., Wendland, W. L., Kuhn, G., eds), pp. 411–420. Berlin Heidelberg New York Tokyo: Springer 1987.

[7] Costabel, M.: Boundary integral operators on Lipschitz domains: elementary results. SIAM J. Math. Anal. *19*, 613–626 (1988).

[8] Costabel, M., Wendland, W. L.: Strong ellipticity of boundary integral operators. J. R. Angew. Math. *372*, 34–63 (1986).

[9] Glowinski, R., Golub, G. H., Meurant, G. A., Periaux, J.: Domain decomposition methods for partial differential equations. Proc. of the 1st International Symposium, Paris, 1987. Philadelphia: SIAM 1988.

[10] Haase, G., Heise, B., Jung, M., Kuhn, M.: FEM⊗BEM - a parallel solver for linear and nonlinear coupled FE/BE-equations. DFG-Schwerpunkt "Randelementmethoden", Report 94–16, University Stuttgart, 1994.

[11] Haase, G., Langer, U.: On the use of multigrid preconditioners in the domain decomposition method. In: Parallel Algorithms for PDEs (Hackbusch, W., ed.), pp. 101–110. Braunschweig: Vieweg 1990.

[12] Haase, G., Langer, U.: The non-overlapping domain decomposition multiplicative Schwarz method. Int. J. Comput. Math. *44*, 223–242 (1992).

[13] Haase, G., Langer, U., Meyer, A.: The approximate dirichlet domain decomposition method. Part I: An algebraic approach. Part II: Applications to 2nd-order elliptic boundary value problems. Computing *47*, 137–151; 153–167 (1991).

[14] Haase, G., Langer, U., Meyer, A.: Domain decomposition preconditioners with inexact subdomain solvers. J. Num. Lin. Alg. Appl. *1*, 27–42 (1992).

[15] Haase, G., Langer, U., Meyer, A., Nepomnyaschikh, S. V.: Hierarchical extension operators and local multigrid methods in domain decomposition preconditioners. East-West J. Numer. Math. *2*, 173–193 (1994).

[16] Hackbusch, W.: Multi-grid methods and applications. Computational mathematics, Vol. 4. Berlin Heidelberg New York: Springer 1985.

[17] Hackbusch, W.: Integralgleichungen: Theorie und Numerik. Stuttgart: Teubner 1989.

[18] Hackbusch, W.: Parallel algorithms for partial differential equations. Proc. of the 6th GAMM-Seminar, Kiel, 1990. Braunschweig: Vieweg 1991.
[19] Haumer, A., Lindner, E. H.: On the optimal design of three-phase asynchronous motors. Institut für Mathematik, Report 485, Johannes Kepler University Linz, 1994.
[20] Heise, B.: Multigrid-Newton methods for the calculation or electromagnetic fields. In: Third Multigrid Seminar, Biesenthal 1988 (Telschow, G., ed.), pp. 53–73. Karl-Weierstrass-Institute, Academy of Sciences, Berlin 1989. Report R-MATH-03/89.
[21] Heise, B.: Mehrgitter-Newton-Verfahren zur Berechnung nichtlinearer magnetischer Felder. Wissenschaftliche Schriftenreihe 4/1991, Technische Universität Chemnitz, 1991.
[22] Heise, B.: Sensitivity analysis for nonlinear magnetic field simulation. In: Modelling uncertain data (Bandemer, H., ed.), pp. 40–45. Berlin: Akademie Verlag 1992.
[23] Heise, B.: Nonlinear field calculations with multigrid-Newton methods. Imp. Comput. Sci. Eng. *5*, 75–110 (1993).
[24] Heise, B: Analysis of a fully discrete finite element method for a nonlinear magnetic field problem. SIAM J. Numer. Anal. *31*, 745–759 (1994).
[25] Heise, B.: Nonlinear magnetic field simulation with FE/BE domain decomposition methods on MIMD parallel computers. DFG-Schwerpunkt "Randelementmethoden", Report 94–19, University Stuttgart, 1994.
[26] Heise, B.: Nonlinear simulation of electro-magnetic fields with domain decomposition methods on MIMD parallel computers. Proceedings of MODELLING 94, Prague, August 29–September 2, 1994. J. Comput. Appl. Math. *63*, 373–381 (1995).
[27] Heise, B.: Nonlinear field simulation with FE domain decomposition methods on massively parallel computers. Surv. Math. Ind. (to appear).
[28] Hsiao, G. C., Wendland, W.: Domain decomposition in boundary element methods. In: Proc. of IV Int. Symposium on Domain Decomposition Methods (Glowinski, R., Kuznetsov, Y. A., Meurant, G., Périaux, J., Widlund, O. B. eds.), pp. 41–49. Philadelphia: SIAM 1991.
[29] Kuhn, M.: A parallel solver for exterior problems based on a coupled FE/BE-model. DFG-Schwerpunkt "Randelementmethoden", Report 94–15, University Stuttgart, 1994.
[30] Langer, U.: Parallel iterative solution of symmetric coupled fe/be- equations via domain decomposition. DFG-Schwerpunkt "Randelementmethoden", Report 92–2, University Stuttgart, 1992. Preprint 217, TU Chemnitz, 1992.
[31] Langer, U.: Parallel iterative solution of symmetric coupled fe/be- equations via domain decomposition. Cont. Math. *157*, 335–344 (1994).
[32] Rjasanow, S.: Vorkonditionierte iterative Auflösung von Randelementgleichungen für die Dirichlet-Aufgabe. Wissenschaftliche Schriftenreihe 7, Technische Universität Chemnitz, 1990.
[33] Steinbach, O., Wendland, W. L.: Efficient preconditioners for boundary element methods and their use in domain decomposition methods. DFG-Schwerpunkt "Randelementmethoden", Report 95-19, University Stuttgart, 1995.
[34] Tong, C. H., Chan, T. F., Kuo, C. J.: A domain decomposition preconditioner based on a change to a multilevel nodal basis. SIAM J. Sci. Stat. Comput. *12*, 1486–1495 (1991).
[35] Wendland, W.: On the coupling of finite elements and boundary elements. In: Discretization methods in structural mechanics (Kuhn, G., Mang, H., eds.), pp. 405–414. Berlin, Heidelberg New York Tokyo: Springer 1990. Proc. IUTUM/IACM Symposium, Vienna, 1989.

B. Heise
M. Kuhn
Institute of Mathematics
Johannes Kepler University Linz
Altenberger Strasse 69
A-4040 Linz, Austria
e-mails: heise@numa.uni-linz.ac.at
kuhn@numa.uni-linz.ac.at